Journal of Institute of Science and Technology, 30(2), 137-150 (2025)
ISSN: 2467-9062 (print), e-ISSN: 2467-9240
https://doi.org/10.3126/jist.v30i2.76472

Research Article

SYNTHESIS OF ZINC OXIDE NANOPARTICLES USING AQUEOUS STEM EXTRACT OF *COLEBROOKEA OPPOSITIFOLIA* Sm: CHRACTERIZATION AND ASSESSMENT OF BIOLOGICAL PROPERTIES

Bimal G. C.*[1], *Indra Ojha* [1], *Pusp Raj Joshi* [2], *Akash Budha Magar*[1], *Sugam Sharma*[3], *Ram Chandra Basnyat*[1], *Khaga Raj Sharma*[1]

[1]*Central Department of Chemistry, Institute of Science and Technology, Tribhuvan University, Kirtipur, Kathmandu, Nepal*

[2]*Annapurna Research Center, Kathmandu, Nepal*

[3]*Department of Computer Engineering, Kathmandu Engineering College, Kathmandu, Nepal*

[*]*Correspondence: khaga.sharma@cdc.tu.edu.np*

***(Received:** April 24, 2025; **Revised:** November 30, 2025; **Accepted:** December 12, 2025)*

ABSTRACT

Colebrookea oppositifolia Sm. is a medicinal shrub traditionally used to treat various ailments, including urinary disorders, skin eruptions, and epilepsy. This study reports the green synthesis of zinc oxide nanoparticles (ZnO NPs) using an aqueous stem extract of *C. oppositifolia* Sm. The synthesized ZnO NPs were characterized by X-ray diffraction (XRD), Fourier transform infrared (FTIR) spectroscopy, ultraviolet-visible (UV-Vis) spectroscopy, field emission scanning electron microscopy (FE SEM), and energy-dispersive X-ray spectroscopy (EDX). UV-Vis analysis of ZnO nanoparticles revealed a peak at 364 nm, while FTIR confirmed the role of plant secondary metabolites in capping, reducing, and stabilizing ZnO NPs. XRD analysis indicated a crystalline structure with an average grain size of 10.89 nm. EDX confirmed the elemental composition of zinc, carbon, and oxygen. The ZnO NPs exhibited strong antibacterial and antifungal activity against *Staphylococcus aureus*, *Shigella sonnei*, and *Candida albicans*. They also demonstrated moderate antioxidant activity and significant anticancer effects against HeLa and A549 cell lines, with IC_{50} values of 56.6 ± 1 µg/mL and 141.0 ± 0.0548 µg/mL, respectively. These findings highlight the potential of *C. oppositifolia* Sm. mediated synthesized ZnO NPs for biomedical, industrial, and packaging applications.

Keywords: Antibacterial, Anticancer, Antioxidant, *Colebrookea oppositifolia* Sm., Nanoparticles

INTRODUCTION

Nanotechnology has contributed to several field of study including drug delivery, material science, and engineering (Pokrajac *et al.*, 2021). Metal oxide nanoparticles are one of the captivating forms of nanomaterials widely used in chemical, biological, and physical science (Fernandez-Garcia *et al.*,2011). They have therapeutic and diagnostic applications in the biomedical sector (Yadav *et al.*, 2021). They have been successfully employed as anode material for fuel cells (Abdalla *et al.*, 2018). The diverse uses and characteristics of metal oxide nanoparticles are responsible for many scientific breakthroughs.

Nanoparticles can be synthesized using chemical precursors, physical forces, or plant extracts. The stability, cost-effectiveness, uniform particle size, seasonal availability of raw materials, and high yield determine the choice of nanoparticle production technique (Pal *et al.*, 2022). Zinc oxide nanoparticles, identified as safe by GRAS (Generally Recognized As Safe), are frequently employed to enhance pharmacophore bioactivity due to their less hazardous and biodegradable nature (Espitia *et al.*, 2016). It has high potential in biomedicine due to its strong thermal and mechanical stability and low toxicity (Bacaksiz *et al.*, 2008). Zinc is an essential trace element required for immune function, enzymatic activity, and cellular growth; its deficiency is associated with impaired development and metabolic dysfunction (Ozgur *et al.*, 2005). Zinc oxide nanoparticles can be produced sustainably by utilizing various plant extracts (Rauf *et al.*, 2019; Shobha *et al.*, 2019). Green synthesis processes are more ecologically benign and sustainable, and they have been used in response to global environmental challenges as well as in the medical field to search for biocompatible drug candidates (Ahmed *et al.*, 2016; Mellinas *et al.*, 2019).

Cancers are the greatest cause of mortality after cardiovascular diseases, accounting for nearly 9.7 million deaths globally in 2022 (Bray *et al.*, 2024).

They are characterized by uncontrolled cell growth, gene mutation, and changes in DNA or RNA. Out of the 20,000 cancer-screened patients, only 6,879 patients survived the battle of cancer in a year (Shilpakar *et al.*,2022). Nepal is seeing a steady increase in the number of cancer patients, and this heartbreaking scenario has become worse every year (Shin *et al.*, 2018). Even though tumor cells are cured by different cancer treatments like surgery, chemotherapy, and radiation therapy, these treatments come with several adverse effects and financial burdens (Peralta-Zaragoza *et al.*, 2012). Zinc oxide nanoparticles show potential as an anticancer treatment as they can specifically target and kill cancer cells. Anticancer activity of ZnO nanoparticles results from the production of reactive oxygen species (ROS), electrostatic interaction, and permeability, as well as retention (EPR) impact towards cancer cells. When ZnO NPs are exposed to the cytoplasmic membrane, the electrostatic interaction of Zn^{+2} generates reactive oxygen species, which develops activity against microbial and fungal species (Mendes *et al.*, 2022).

C. oppositifolia Sm. (locally known as Dhursul), is a shrub used to cure wounds, urinary problems, skin eruptions, nose bleeding, and epilepsy (Sharma *et al.*, 2021). Many secondary metabolites from this plant, including polyphenols, alkaloids, and flavonoids, operate as antioxidants, antifertility agents, antiulcer, antibacterial agents, and antifungal agents (Ajaib *et al.*, 2018). These metabolites are involved in the treatment of several diseases (Viswanath *et al.*, 2021). To the best of our knowledge, this study is the first to report the green synthesis of ZnO NPs using the aqueous stem extract of *C. oppositifolia*, introducing a previously unutilized plant source for eco-friendly nanoparticle fabrication. The study offers a comprehensive physicochemical characterization of the synthesized zinc oxide nanoparticles using multiple analytical techniques, ensuring a detailed understanding of their structural, morphological, and elemental properties. A key strength of this research is the simultaneous evaluation of four major bioactivities**.**

The primary objective of this research is to synthesize zinc oxide nanoparticles (ZnO NPs) using a green approach with plant extracts and to characterize them using UV-Vis spectroscopy, Fourier-transform infrared spectroscopy (FTIR), X-ray diffraction (XRD), field emission scanning electron microscopy (FE-SEM), and energy-dispersive X-ray spectroscopy (EDX). Furthermore, the study aims to evaluate the antimicrobial, antifungal, anticancer, and antioxidant properties of the synthesized ZnO nanoparticles, highlighting their potential applications in biomedical and pharmaceutical fields.

MATERIALS AND METHODS

Chemicals and Equipment

For the entire experiment, deionized water was used. Microplate reader (Epoch 2, Biotek, Instruments, Inc., USA), Azure biosystems microplate spectrophotometer, water bath (Clifton), Analytical grade zinc acetate dehydrate (Merck), ethanol, and NaOH (LOBA CHEMIE), pH meter (Nike), DPPH reagents (Merck), Muffle Furnace (Accuma X India) were employed in the study. Muller Hinton Broth (MHB), Muller Hinton Agar (MHA), and Neomycin were brought from HiMedia Pvt. Ltd, India.

Plant Collection and Identification

Plant samples were collected from the Doti district of Nepal (Latitude 29.3739° N and Longitude 80.9748° E) in their natural environment. The plant was recognized as having significant medicinal value by the local people. It was collected in May of 2023 and was identified by a taxonomist at the Godawari, Lalitpur, Nepal, as *C. oppositifolia* Sm. with voucher code BGc01 KATH163317. The photograph of the fresh plant is shown in Figure 1.

Figure 1. *Colebrookea oppositifolia* Sm.

Preparation of Plant Extracts

After cleaning plants were sliced, chopped, and shade-dried, the stems of the plant were crushed into a powder and then kept in airtight plastic bags for later use. Firstly, 10 g of finely ground stem powder was added to 200 mL of deionized water taken in a conical flask, and heated to 50°C for one hour while being continuously swirled with a magnetic hot plate stirrer. The contents were filtered through Whatman filter paper (no.1), and the filtrate was taken as the plant extract.

Synthesis of Zinc Oxide Nanoparticles

Nanoparticles of zinc oxide were produced by slightly modifying the standard protocol in which 10 mL of aqueous extract with an initial pH of 5.28 was added to 200 mL of 0.02 mM zinc acetate dihydrate solution

(Fakhri *et al.*, 2019). NaOH solution was added to maintain the pH 11. A solid, yellowish-white mixture solution was generated after two hours of stirring, then absorbance was measured using a UV-visible spectrophotometer. Then, the solution was centrifuged for 30 min at 9000 rpm and rinsed with ethanol and distilled water. Thus, the obtained solid products were calcinated at 600 °C for a couple of hours in a muffle furnace. The nanoparticles were stored in an Eppendorf tube for further analysis.

UV-Visible and FTIR Spectroscopy

The peak in the range of 300-600 nm region was measured to confirm the synthesis of ZnO nanoparticles. The measurement was taken with a UV-visible spectrometer (SPECORD 200 PLUS). The functional groups in the organic compounds from plant extracts were recognized by FTIR (Shimadzu IR Tracer100). Origin 2019b (9.5) was used to construct FTIR spectra.

XRD Analysis

An X-ray diffractometer (D2phaser, Bruker, located at NAST, Nepal) operating at 30 kV with a Cu Kα radiation source (λ =1.540 Å) was used to examine the crystal structures of nanoparticles. 2θ scan was performed between 20° to 80°, and Origin 2019b (9.65) was used to analyze the data. The Debye Scherrer equation was utilized for calculating size.

$$D = \frac{K\lambda}{\beta\cos\theta} \quad \ldots (1)$$

where, λ = wavelength of X-ray, D = crystallite size, k = Scherrer constant, and β = Full-width half maximum.

FE-SEM and EDX Analysis

High-resolution features such as size, composition, and other chemical characteristics of nanoparticles were studied using field emission-scanning electron microscopy (FE-SEM) (SU-70 apparatus, Korea) and EDX (Oxford instruments). The diameters of the synthesized nanoparticles were measured with the help of ImageJ software.

Antioxidant Potential

The DPPH assay, which was carried out with a few small adjustments to the standard procedure, measured the antioxidant activity (Shrestha *et al.*, 2024). The 96-well plate was filled with 100 µL of extract, and an initial reading was noted at 517 nm. Then, 100 µL of DPPH was added, and the final concentration was recorded. As the compound released electrons, the solution turned from deep violet to yellow, indicating the reduction of the compound.

$$\%\ \text{inhibition} = \frac{A_{control} - A_{sample}}{A_{control}} \quad \ldots (2)$$

Where, $A_{control}$ = Absorbance of the control, A_{sample} = Absorbance of the sample. The inhibition curve was used to deduce IC_{50} values. The curve was plotted by graphing the extract concentration against the corresponding scavenging effect.

Antibacterial Activity

The microorganisms used in the study were ATCC 700603 *Klebsiella pneumoniae,* ATCC 43300 *Staphylococcus aureus*, ATCC 25931 *Shigella sonnei,* and ATCC 25912 *Escherichia coli.* The Institute of Biomolecule Reconstruction at Sun Moon University in the Republic of Korea donated these strains.

To evaluate the antibacterial activity, a modified agar well diffusion assay was carried out (Balouiri *et al.*, 2016). Bacteria were cultured in Muller-Hinton broth (MHB). Similarly, Muller-Hinton agar (MHA) was taken to measure antibacterial activity. A 100 µL of 0.5 standard inoculum was made a carpet lawn on MHA plates. Well diffusion method was done on MHA plates, where 50 µL ZnO NPs disperssed samples were placed in the wells with a positive control (neomycin) and a negative control (50% DMSO) was also kept. The plates were incubated for 24 hours at 37°C. Then Zone of inhibition (ZOI) was measured.

Antifungal Activity

A modified Agar well diffusion technique evaluated antifungal activity against ATCC 10231 *Candida albicans* (Ahmed *et al.*, 2016). Fungal spore suspensions of 100 µL were spreaded onthe plates. For agar diffusion method the samples of a standard 5 mg/mL kanamycin solution (10 µL) were added. ZOI was measured to evaluate the antifungal properties after 24 hours of incubation at 37°C.

MTT Assay

A549 (lung cancer) and HeLa (cervical cancer) cell lines were cultured in T flasks supplemented with Dulbecco's Modified Eagle Medium (DMEM) inside a 5% CO_2 incubator. L-glutamine 1% and penicillin/streptomycin 1% were added as antibiotics. As a nutrient supplement 10% of fetal bovine serum (FBS) was also added.

ZnO nanoparticles-treated cells were tested for cell

viability using a modification of the MTT assay (Mosmann, 1983). The procedure involved seeding 100 µL of media containing 1 x 10^4 cells/well onto a microplate and enabling the cells to remain attached for a full day in a 5% CO_2 incubator (37°C). The medium was removed, and different concentrations of samples were added to the wells, and the plate was incubated for 48 hours. Afterward, the supernatant was removed. Each well received 100 µL of media containing 20 µL of MTT (3- [4, 5-dimethylthiazole-2-yl]-2, 5- diphenyl-tetrazolium bromide), which was then incubated for four hours into the incubation period, and finally the purple formazan product was generated. This product was dissolved for 4 hours. DMSO 0.1% (100 µL) was added to dissolve formazan crystals, which were allowed to settle. Finally, absorbance readings were noted at 570 nm and 630 nm. Positive controls for cisplatin and doxorubicin cell lines A549 and HeLa cell lines were used accordingly. The cytotoxic activity was measured using the following equation:

$$\% \text{ cytotoxic activity} = \frac{Abs1 - Abs2}{Abs_1} \times 100 \ldots (3)$$

Where Abs_1 and Abs_2 are the absorbance of the control and treated samples.

Statistical Analysis

IC_{50} was calculated through the software Graph Pad Prism 9.5.1. UV, FTIR, and XRD spectra were plotted using Origin 2019b (9.65) software. SEM images were analyzed through the software ImageJ.

RESULTS AND DISCUSSION

UV- Vis Spectroscopy

The green-brownish color of the reaction mixture shifted to white, indicating the presence of zinc nanoparticles (Jiang *et al.*, 2018; Singh *et al.*, 2019). When zinc acetate was added to stem extracts in the presence of NaOH, absorption occurred in the 300-500 nm range (Akhil & Khan, 2017). The maximal absorption peak at 364 nm was detected in the plant-assisted synthesis of ZnO NPs, as shown in Figure 2(a), which was consistent with the findings of the earlier investigation (Acharya *et al.*, 2024). These peaks result from the transfer of electrons from the valence band to the conduction band associated with surface plasmon resonance (Zak *et al.*, 2011). Synthesized zinc oxide nanoparticles displayed stability within 0 hours to 24 hours. The UV-visible spectra of plant extract and nanoparticle dispersions are provided in Figure 2(a). Band gap energy of ZnO NPs was calculated using Planck's equation, in which the wavelength (364 × 10^{-7} m) is represented by λ and the Planck constant (4.136 × 10^{-15} eV) is designated by h. The ZnO NPs, with the assistance of plants, turned out to have an energy of 3.41 eV, which is consistent with previous findings (Yassin *et al.*, 2023).

Fourier Transform Infrared Spectroscopy (FTIR)

The FTIR spectra of nanoparticles and aqueous extracts are provided in Figure 2(b). The phytochemicals in *C. oppositifolia* Sm. aqueous stem extract has functional groups that can reduce, cap, and stabilize zinc oxide nanoparticles. The differences in peak positions and peak intensities for a particular functional group in the spectra of plant extract and nanoparticle confirm their involvement in the nanoparticle synthesis process (Abraham *et al.*, 2020). A distinctive peak was detected in the FTIR spectra at roughly 669 cm^{-1}, which may have resulted from ZnO nanostructure stretching (Naseer *et al.*, 2020). The vibrational peaks around 3670 cm^{-1} in the plant extract, representing hydroxyl (OH) groups, have shifted to 3728 cm^{-1} in ZnO NPs. This peak indicates -OH stretching vibration in alcoholic and phenolic compounds, suggesting their role in nanoparticle synthesis. The wide C-H stretching peak at 2989 cm^{-1} in the plant extract has moved to 2916 cm^{-1} in ZnO NPs. The peak at 1392 cm^{-1} in ZnO NPs appears at 1390 cm^{-1} in the plant extract. These spectra were found to be similar to the previous finding (Chabattula *et al.*, 2021; Faisal *et al*., 2021).

X-ray Diffraction (XRD)

Sharp and narrow diffraction peaks in the XRD pattern confirm the crystallinity of the synthesized nanoparticles (Khoshhesab *et al.*, 2011). Distinct peaks corresponding to Miller indices of (100), (002), (101), (102), (110), (103), (112), and (201) are visible in the XRD pattern of ZnO NPs provided in Figure 2(c). The diffraction peaks appear at 2θ angles of 31.54, 34.2, 36.02, 47.32, 56.4, 62.68, and 68.71, which are in excellent agreement with the standard hexagonal wurtzite structure of ZnO (JCPDS file number 36-1451) (Naseer *et al.*, 2020). The strong diffraction corresponds to the (101) plane. Such a crystalline wurtzite structure has also been previously reported for green-synthesized ZnO NPs (Arakha *et al.*, 2015). The crystallite size was calculated as 10.89 nm with the help of the Debye-Scherrer equation. This value is very close to 12.79 nm reported for ZnO NPs synthesized using an aqueous extract of *Polystichum lentum* (Shrestha *et al.*, 2024). FE-SEM images provide information about the morphology of nanoparticles, whereas XRD provides information about grain size and crystallinity (He *et al.*, 2018; Zhou *et al.*, 2016).

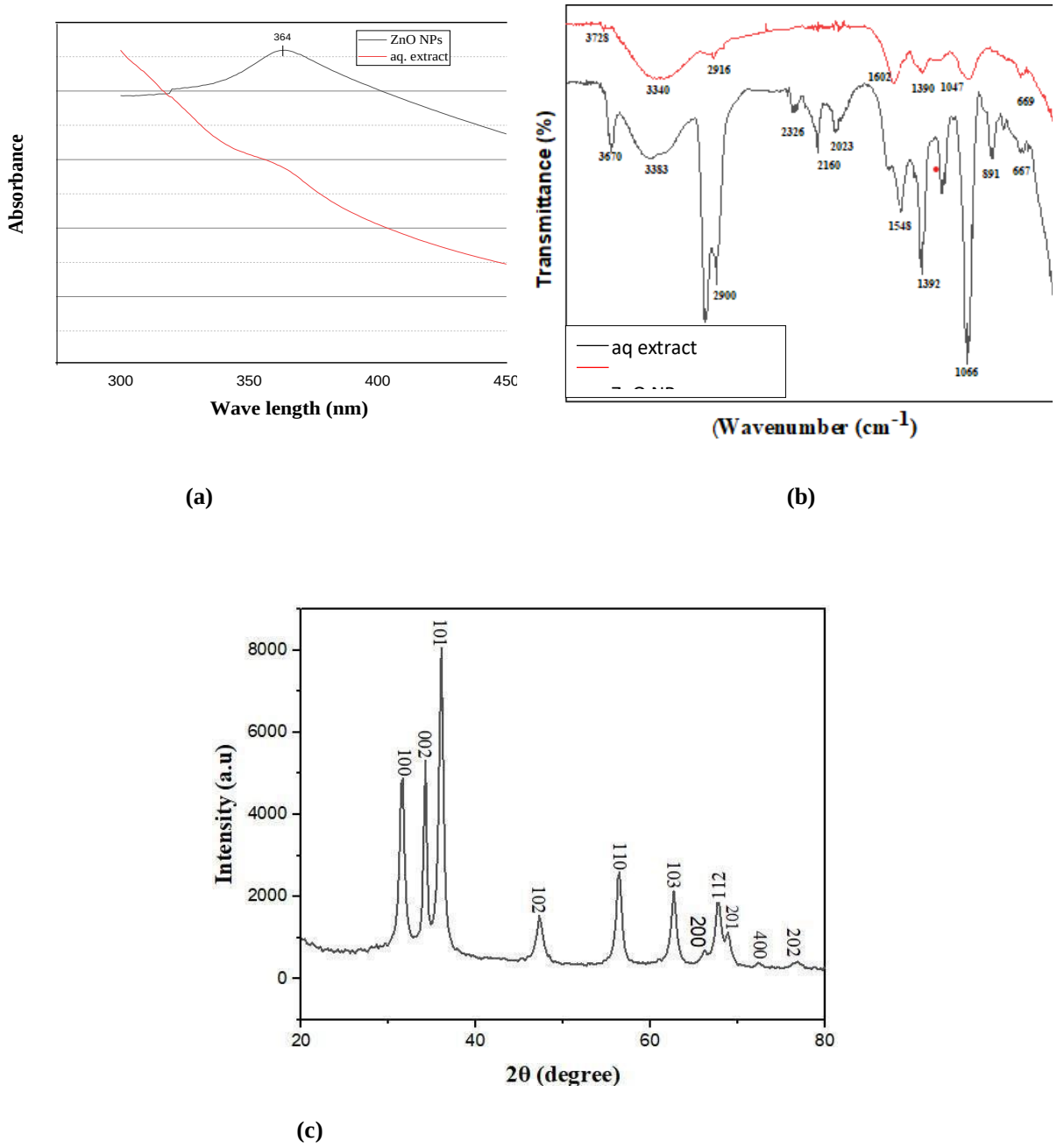

Figure 2(a). UV spectra of stem extract assisted ZnO NPs and aq. stem extract. (b) FTIR spectra of aqueous extract and assisted ZnO NPs. and (c) XRD pattern of plant-assisted ZnO NPs.

Field Emission Scanning Electron Microscopy (FE-SEM)

FE-SEM analysis was carried out to study the morphology, size, and shape of the particles. Its image is analyzed in the different resolutions of 200 nm, 400 nm, and 300 nm. Meanwhile, ZnO NPs displayed irregular shapes with an average diameter of 78.01 nm. The electrostatic interaction and hydrogen bonding between the plant's secondary metabolites and nanoparticles facilitated the formation of FE-SEM clustered images (Priya *et al.*,2011). The FE-SEM images and histogram showing particle size distribution are provided in Figure 3(a,b,c,d).

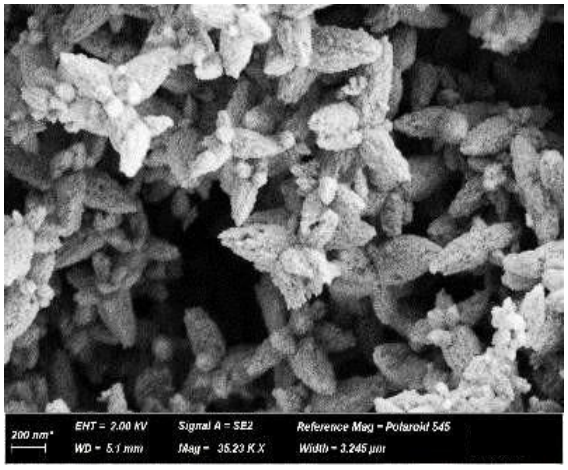

(a)

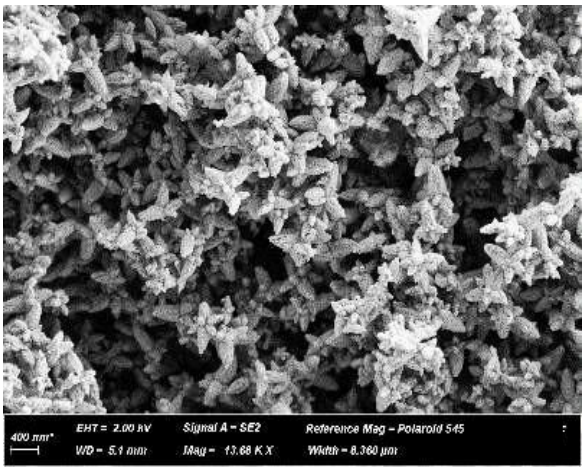

(b)

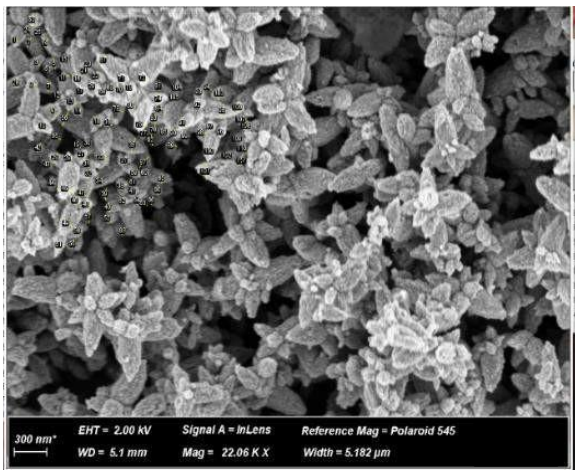

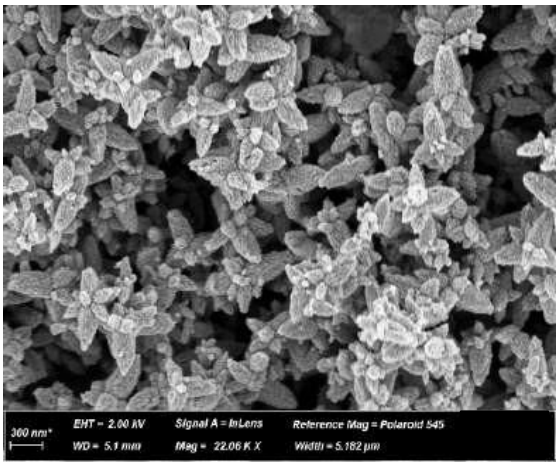

(c)

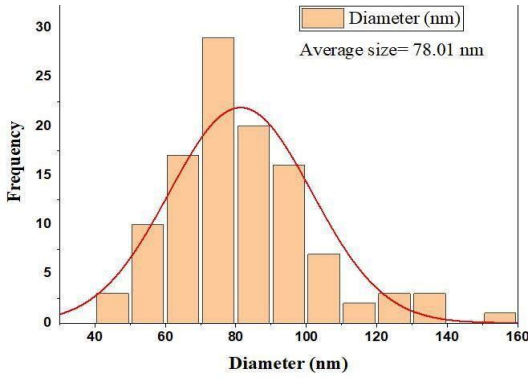

(d)

Figure 3. FE-SEM images of ZnO NPs. (a) at a resolution of 200 nm, (b) at a resolution of 400 nm, (c) at a resolution of 300 nm, (d) Size distribution of ZnO NPs.

EDX Analysis

Figures 4(a) and 4(b) illustrate the elemental mapping and EDX spectrum of ZnO NPs, respectively, revealing characteristic zinc peaks at 9.6, 8.6, and 1 keV. Multiple peaks are caused by the diffraction of different electrons from the zinc atom, while additional peaks at 0.3 keV and 0.5 keV represent the presence of carbon and oxygen. Their appearance is caused by surface-adsorbed plant metabolites (Shrestha *et al.*, 2024). These observations align with earlier reports (Barzinjy & Azeez, 2020).

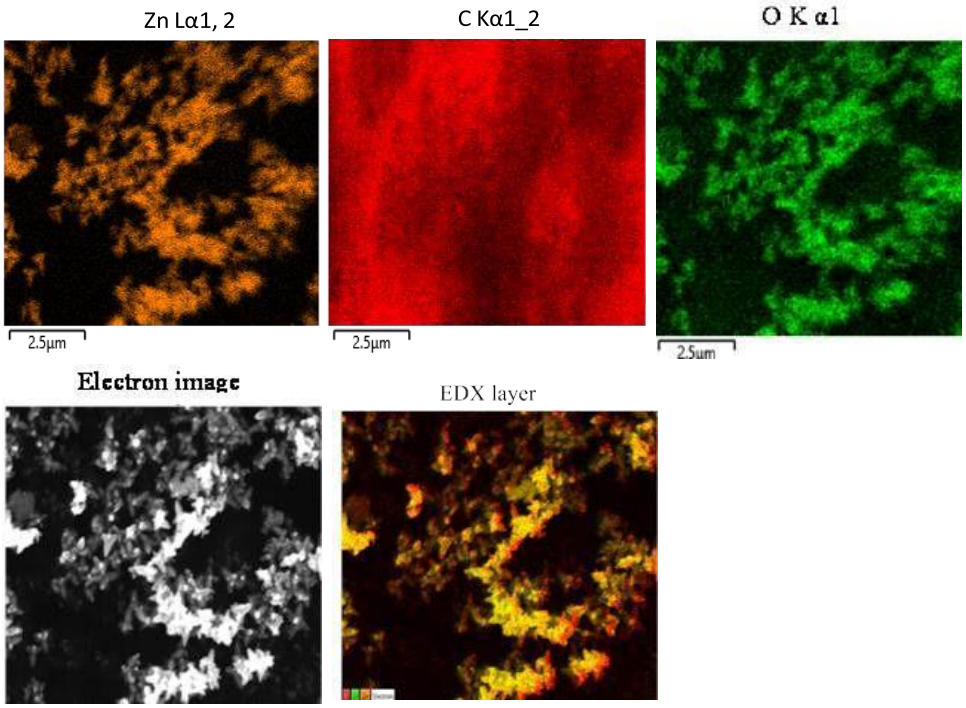

(a)

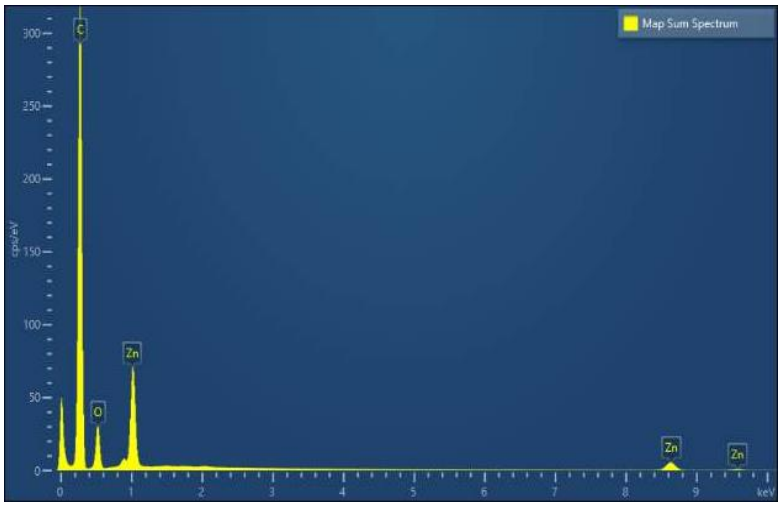

(b)

Figure 4(a). Color mapping of ZnO NPs. (b) EDX spectrum of ZnO NPs.

Antibacterial Activity

Table 1 presents the ZOI of aqueous extract and nanoparticles against test organisms. The photographs of Petri plates are provided in Figure 5, whereas Figure 6 is a comparative presentation of antibacterial activity.

Table 1. Antibacterial activity of aqueous stem extracts and ZnO NPs against four bacterial strains.

Sample	Zone of inhibition (mm)			
	K. pneumonia	***S. sonnei***	***S. aureus***	***E. coli***
Stem aqueous extract	18	17	15	9
ZnO NPs	10	19	20	9
Neomycin	24	28	30	22

Zinc oxide nanoparticles were more efficient against *S. aureus* and *S. sonnei* than *K. pneumoniae* and *E. coli*. Aqueous extract of the stem showed ZOI of 15 mm against *S. aureus*, whereas ZnO NPs showed ZOI of 20 mm. Similarly, the aqueous stem extract showed a ZOI of 17 mm against *S. sonnei*, and 19 mm was recorded for ZnO NPs. The ZnO NPs' antimicrobial activity is supported by the previous findings (Arakha *et al.*, 2015; Shrestha *et al.*, 2024). The antibacterial activity of ZnO NPs against *E. coli* was equal to that of the plant extract, whereas the activity was lower against *K. pneumoniae.*

Zinc oxide nanoparticles, while non-lethal at low concentrations, can become deadly at higher concentrations. They can become hazardous at greater concentrations, which could be dangerous for the environment and human health (Kahru & Dubourguier, 2010). The ecosystem may be impacted by the careless disposal of these nanoparticles. To prevent this, a safe and effective method of disposal is to heat the nanoparticles with carbon. The outcome of this procedure is the development of metallic zinc and carbon monoxide gas, which can be controlled and managed. The zinc oxide is converted to metallic zinc, which can be safely recycled or reused, reducing the risk of environmental pollution and contributing to sustainable practices (Wu *et al.*, 2019)

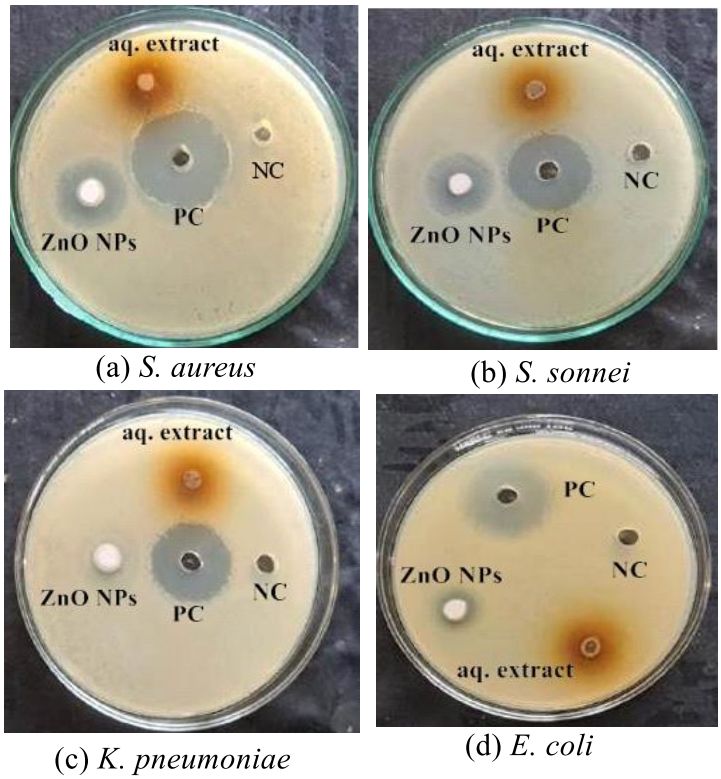

Figure 5. ZnO NPs and aqueous extract showed antibacterial activity against (a*) S. aureus,* (b) *S. sonnei,* (c) *K. pneumoniae* (d) *E. coli.*

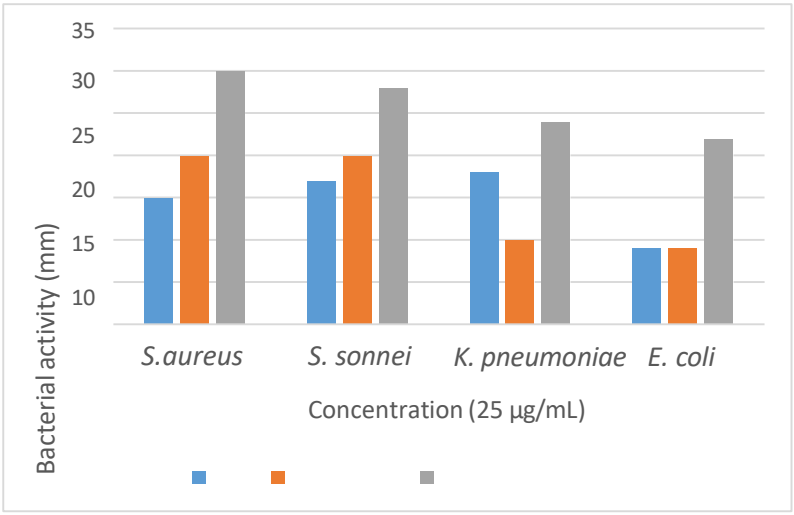

Figure 6. Aqueous extract (aq.) and ZnO NPs, antibacterial activity against bacterial strains.

Antifungal Potential

The antifungal activity of ZnO NPs against *C. albicans* is shown in Figure 7. The positive control showed a ZOI of 25 mm, whereas ZnO NPs showed a slightly lower ZOI of 19 mm. A previous study on ZnO nanoparticles has reported a ZOI of 11.4 mm (Sharma & Ghose, 2015). The inhibition of growth of the *C. albicans* fungus was probably caused by the small dimensions of nanoparticles, which allowed them to pass through the cell walls of fungi (Sharma & Ghose, 2015). It resulted in the blockage of the fungal cell activity, growth inhibition, and death (Slavin & Bach, 2022).

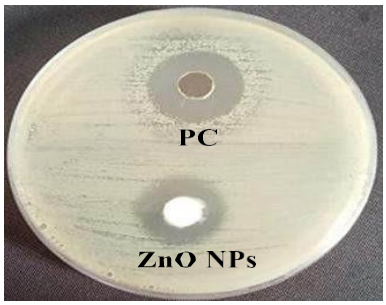

Figure 7. Antifungal activity of ZnO NPs against *C. albicans*.

Antioxidant Potential

The present investigation found a concentration-dependent increment in the antioxidant activity of nanoparticles, as demonstrated in Figure 8. ZnO nanoparticles showed significant antioxidant activity; however, the IC_{50} values for the ZnO NPs (109.1 ± 0.53 µg/mL) were higher than that of standard quercetin (3.36 ± 1.03 µg/mL). The antioxidant potential of ZnO nanoparticles could be accounted for by the large surface area of nanoparticles and the presence of antioxidant plant metabolites adsorbed on the surface of nanoparticles. Mechanism of antioxidant activities may involve the transfer of a single electron, hydrogen, or metal chelation (Bhusal *et al.*, 2024; Lu *et al.*, 2010).

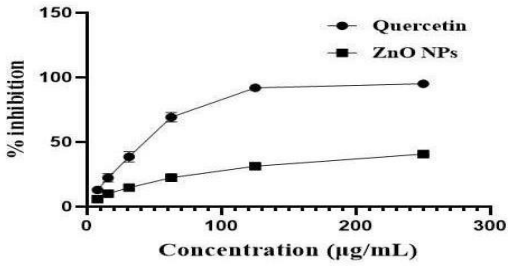

Figure 8. Inhibition shown by ZnO NPs and standard quercetin.

Cytotoxicity

The findings demonstrated that ZnO nanoparticles (ZnO NPs) exhibit significant anticancer potential. At a concentration of 200 µg/mL, ZnO NPs induced mortality rates of 67.53% in HeLa cells and 59.40% in A549 cells. The calculated IC_{50} values were 56.6 ± 1 µg/mL for HeLa cells and 141.0 ± 0.0548 µg/mL for A549 cells, indicating a promising therapeutic

potential for cancer treatment. This is further supported by the IC_{50} value of standard doxorubicin for HeLa cells (71.51 ± 0.418 µg/mL) and cisplatin for A549 cells (55.56 ± 0.280 µg/mL). The anticancer activity of ZnO NPs followed a concentration-dependent profile, as illustrated in Figures 9(a)–9(j), which aligns with previous studies (Perumal *et al.*, 2024). The cytotoxic effects of ZnO NPs are attributed to their ability to impair mitochondrial function, generate intracellular reactive oxygen species (ROS), and induce apoptosis, ultimately disrupting cancer cell viability and highlighting their potential as a promising anticancer agent (Huang *et al.*, 2017).

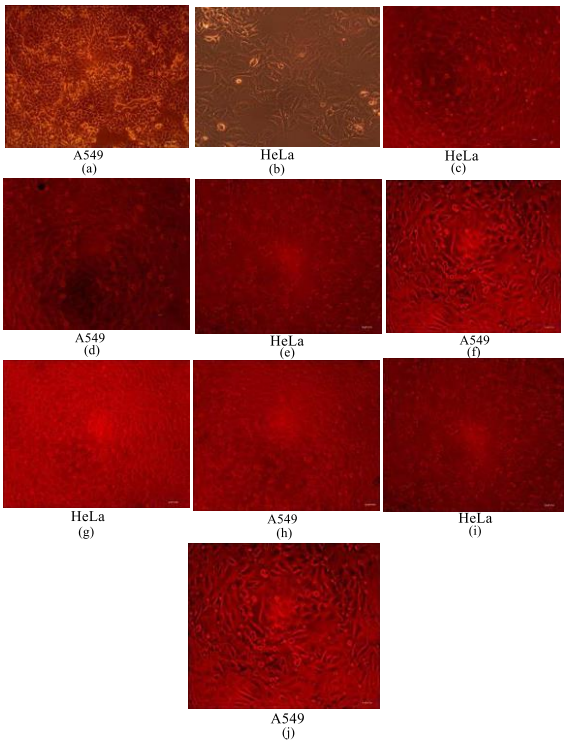

Figure 9. (a) Untreated cell lines of A549, (b) Untreated cell lines of HeLa, (C) Cell lines treated after 48 hours with 200 µg/mL of ZnO NPs in HeLa (d) Cell lines treated after 48 hours with 200 µg/mL of ZnO NPs. in A549, (e) Cell lines treated after 48 hours with 100 µg/mL of ZnO NPs. in HeLa (f) Cell lines treated after 48 hours with 100 µg/mL of ZnO NPs. in A549, (g) Cell lines were treated after 48 hours with 50 µg/mL of ZnO NPs. in HeLa, (h) Cell lines were treated after 48 hours with 50 µg/mL of ZnO NPs. in A549 cell, (i) Cell lines were treated after 48 hours with 25 µg/mL of ZnO NPs. in HeLa cell lines, (j) Cell lines were treated after 48 hours with 50 µg/mL of ZnO NPs. in A549 cell lines.

CONCLUSIONS

In this study, an aqueous extract of *C. oppositifolia* Sm. was utilized for the green synthesis of zinc oxide nanoparticles (ZnO NPs). The synthesized ZnO NPs exhibited a hexagonal wurtzite crystal structure with a non-uniform size distribution. They demonstrated moderate antioxidant activity and enhanced antibacterial efficacy against both Gram-positive and Gram-negative bacteria. Additionally, the ZnO NPs exhibited significant antifungal properties against *C. albicans* and potent anticancer activity against HeLa and A549 cancer cell lines. These findings highlight the potential of plant-assisted ZnO NPs as a promising therapeutic agent for bacterial and fungal infections, as well as cancer treatment. Further investigations into their mechanism of action and in vivo efficacy could pave the way for their biomedical applications.

ACKNOWLEDGMENTS

The plant identification was made possible by the National Herbarium and Plant Laboratories, Godawari, Lalitpur, Nepal, to which the author thanked. The XRD data were provided by the Nepal Academy of Science and Technology (NAST), Lalitpur, Nepal, and are gratefully acknowledged by the authors. The bacterial strains were provided by the Institute of Biomolecule Reconstruction at Sun Moon University in the Republic of Korea. The authors express sincere thanks to Jeonbuk National University, Republic of Korea, for providing FE-SEM and EDX images.

AUTHORS CONTRIBUTION

Conceptualization: IO, KRS, RCB; Investigation: BGC; Methodology: BGC; Data curation: KRS, SS; Data analysis: BCG, KRS, SS; Writing - original draft: BGC; Writing - review and editing: ABM, IO, KRS, PRJ.

CONFLICT OF INTEREST

There is no conflict of interest among the authors regarding the publication of this research paper in all issues.

DATA AVAILABILITY

The data regarding this research paper will be provided on request.

FUNDING STATEMENT

This research was conducted solely through the efforts of the authors and is not supported by any agency or organization.

REFERENCES

Abdalla, A. M., Hossain, S., Azad, A. T., Petra, P. M. I., Begum, F., Eriksson, S. G., & Azad, A.
K. (2018). Nanomaterials for solid oxide fuel cells: A review. *Renewable and Sustainable Energy Reviews*, 82, 353–368. https://doi.org/10.1016/j.rser.2017.09.046.

Abraham, J., Jose, B., Jose, A., & Thomas, S. (2020). Chapter 2 - Characterization of green nanoparticles from plants (pp. 21-39). In Thajuddin, N. & Mathew, S. (Eds.), *Phytonanotechnology*. Elsevier. https://doi.org/10.1002/9783527834143.ch9.

Acharya, R., Tettey, F., & Gupta, A. (2024). Bioinspired synthesis and characterization of zinc oxide nanoparticles and assessment of their cytotoxicity and antimicrobial efficacy. *Discover Applied Sciences*, 6, 85. https://doi.org/10.1007/s42452-024-05719-2.

Ahmed, S., Ahmed, M., Swami, B. L., & Ikram, S. (2016). A review on plant extract-mediated synthesis of silver nanoparticles for antimicrobial applications: A green expertise. *Journal of Advanced Research*, 7(1), 17–28. https://doi.org/10.1016/j.jare.2015.02.007.

Ahmed, S., Saifullah, Ahmad, M., Swami, B. L., & Ikram, S. (2016). Green synthesis of silver nanoparticles using *Azadirachta indica* aqueous leaf extract. *Journal of Radiation Research and Applied Sciences*, *9*(1), 1–7. https://doi.org/10.1016/j.jrras.2015.06.006.

Ajaib, M. A. M., Abid, S. A. S., Anjum, M. A. M., Noshad, Q., Siddiqui, M. F., & Iqbal, M. F. (2018). Phytochemical, antibacterial, and antifungal activities of leaves and bark of *Colebrookea oppositifolia*: an ethnomedicinal plant. *Pure and Applied Biol*ogy, 7(1), 138-151. http://dx.doi.org/ 10.19045/bspab.2018.70017.

Akhil, K., & Khan, S. S. (2017). Effect of humic acid on the toxicity of bare and capped ZnO nanoparticles on bacteria, algal, and crustacean systems. *Journal of Photochemistry and Photobiology B: Biology*, 167, 136–149. https://doi.org/10.1016/j.jphotobiol.2016.12.010.

Arakha, M., Saleem, M., Mallick, B. C., & Jha, S. (2015). The effects of interfacial potential on the antimicrobial propensity of ZnO nanoparticles. *Scientific Reports*, 5(1), 9578. https://doi.org/10.1038/srep09578.

Bacaksiz, E., Parlak, M., Tomakin, M., Ozcelik, A., Karakiz, M., & Altunbas, M., (2008). The effects of zinc nitrate, zinc acetate, and zinc chloride precursors on the investigation of structural and optical properties of ZnO thin films. *Journal of Alloys and Compounds*, 466(1), 447–450. https://doi.org/10.1016/j.jallcom.2007.11.061.

Balouiri, M., Sadiki, M., & Ibnsouda, S. K. (2016). Methods for in vitro evaluating antimicrobial activity: A review. *Journal of Pharmaceutical Analysis*, 6(2), 71–79. https://doi.org/10.1016/j.jpha.2015.11.005.

Barzinjy, A. A. & Azeez, H. H. (2020). Green synthesis and characterization of zinc oxide nanoparticles using *Eucalyptus globulus* Labill. Leaf extract and zinc nitrate hexahydrate salt. *SN Applied Sciences*, 2(5), 991. https://doi.org/10.1007/s42452-020-2813-1.

Bhusal, M., Sharma, K., Magar, A. B., Pant, J., & Sharma, K. R. (2024). Chemical analysis and biological activities on solvent extracts from different parts of *Rhus chinensis* Mill. *Natural product research*, 1–7. Advance online publication. https://doi.org/10.1080/14786419.2024.2387831.

Bray, F., Laversanne, M., Sung, H., Ferlay, J., Siegel, R. L., Soerjomataram, I., & Jemal, A. (2024). Global cancer statistics 2022: GLOBOCAN estimates of incidence and mortality worldwide for 36 cancers in 185 countries. *CA: a cancer journal for clinicians*, *74*(3), 229–263. https://doi.org/10.3322/caac.21834.

Chabattula, S. C., Gupta, P. K., Tripathi, S. K., Gahtori, R., Padhi, P., Mahapatra, S., & Biswal, B.

K. (2021). Anticancer therapeutic efficacy of biogenic *Am*-ZnO nanoparticles on 2D and 3D tumor models. *Materials Today Chemistry*, 22, 100618. https://doi.org/10.1016/j.mtchem.2021.100618.

Espitia, P. J. P., Otoni, C. G., & Soares, N. F. F. (2016). Chapter 34 - Zinc oxide nanoparticles for food packaging applications (pp. 425-431). In Barros-Velázquez, J. (Ed.), *Antimicrobial Food Packaging*. San Diego: Academic Press. https://doi.org/10.1016/B978-0-12-800723-5.00034-6.

Faisal, S., Jan, H., Shah, S. A., Shah, S., Khan, A., Akbar, M. T., Rizwan, M., Jan, F., Wajidullah, Akhter, N., Khattak, A., & Syed, S. (2021). Green synthesis of zinc oxide (ZnO) nanoparticles using aqueous fruit extracts of *Myristica fragrans*: Their characterizations and biological and environmental applications. *ACS Omega*, 6(14), 9709–9722. https://doi.org/10.1021/acsomega.1c00310.

Fernández-García, M. & Rodriguez, J. A. (2011). Metal oxide nanoparticles. In *Encyclopedia of Inorganic and Bioinorganic Chemistry*. John Wiley & Sons. https://doi.org/10.1002/9781119951438.eibc0331.

He, K., Chen, N., Wang, C., Wei, L., & Chen, J. (2018). Method for determining crystal grain size by X-ray diffraction. *Crystal Research and Technology*, 53(2), 1700157. https://doi.org/10.1002/crat.201700157.

Huang, X., Zheng, X., Xu, Z., & Yi, C. (2017). ZnO-based nanocarriers for drug delivery application: From passive to smart strategies. *International Journal of Pharmaceutics*, 534(1), 190–194. https://doi.org/10.1016/j.ijpharm.2017.10.008.

Jiang, J., Pi, J., & Cai, J. (2018). The advancing of zinc oxide nanoparticles for biomedical applications. *Bioinorganic Chemistry and Applications*, 2018, 1062562. https://doi.org/10.1155/2018/1062562.

Kahru, A., & Dubourguier, H. C. (2010). From ecotoxicology to nanoecotoxicology. *Toxicology*, *269*(2-3), 105–119. https://doi.org/10.1016/j.tox.2009.08.016.

Khoshhesab, Z. M., Sarfaraz, M., & Asadabad, M. A. (2011). Preparation of ZnO nanostructures by chemical precipitation method. *Synthesis and Reactivity in Inorganic, Metal-Organic, and Nano-Metal Chemistry*, 41(7), 814–819. https://doi.org/10.1080/15533174.2011.591308.

Lü, J. M., Lin, P. H., Yao, Q., & Chen, C. (2010). Chemical and molecular mechanisms of antioxidants: experimental approaches and model systems. *Journal of cellular and molecular medicine*, *14*(4), 840–860. https://doi.org/10.1111/j.1582-4934.2009.00897.x.

Mellinas, C., Jiménez, A., & Garrigós, M. C. (2019). Microwave-assisted green synthesis and antioxidant activity of selenium nanoparticles using *Theobroma cacao* L. bean shell extract. *Molecules*, 24(22), 22. https://doi.org/10.3390/molecules24224048.

Mendes, C. R., Dilarri, G., Forsan, C. F., Sapata, V. M. R., Lopes, P. R. M., Moraes, P B., Montagnolli, R. N., Ferreira, H., & Bidoia, B. D. (2022). Antibacterial action and target mechanisms of zinc oxide nanoparticles against bacterial pathogens. *Scientific Reports*, 12(1), 2658. https://doi.org/10.1038/s41598-022-06657-y.

Mosmann T. (1983). Rapid colorimetric assay for cellular growth and survival: application to proliferation and cytotoxicity assays. *Journal of immunological methods*, *65*(1-2), 55–63. https://doi.org/10.1016/0022-1759(83)90303-4.

Naseer, M., Aslam, U., Khalid, B., & Chen, B. (2020). Green route to synthesize Zinc oxide nanoparticles using leaf extracts of *Cassia fistula* and *Melia azadarach* and their antibacterial potential. *Scientific Reports*, 10(1), 9055. https://doi.org/10.1038/s41598-020-65949-3.Özgür, Ü., Alivov,Y. I., Liu C., Teke, A., Reshchikov, M. A., Dogan, S., Avrutin, V., Cho, S. J., & Morko, H. (2005). A comprehensive review of ZnO materials and devices. *Journal of Applied Physics*, 98(4), 041301. https://doi.org/10.1063/1.1992666.

Pal, K., Chakroborty, S., & Nath, N. (2022). Limitations of nanomaterials insights in green chemistry sustainable route: Review on novel applications. *Green Processing and Synthesis*, 11(1), 951–964. https://doi.org/10.1515/gps-2022-0081.

Peralta-Zaragoza, O., Bermúdez-Morales, V. H., Pérez-Plasencia, C., Salazar-León, J., Gómez-Cerón, C., & Madrid-Marina, V. (2012). Targeted treatments for cervical cancer: a review. *OncoTargets and therapy*, *5*, 315–328.

https://doi.org/10.2147/OTT.S25123.

Perumal, P., Sathakkathulla, N. A., Kumaran, K., Ravikumar, R., Selvaraj, J. J., Nagendran, V., Gurusamy, M., Shaik, N., Gnanavadivel Prabhakaran, S., Suruli Palanichamy, V., Ganesan, V., Thiraviam, P. P., Gunalan, S., & Rathinasamy, S. (2024). Green synthesis of zinc oxide nanoparticles using aqueous extract of shilajit and their anticancer activity against HeLa cells. *Scientific reports*, *14*(1), 2204. https://doi.org/10.1038/s41598-024-52217-x.

Pokrajac, L., Abbas, A., Chrzanowski, W., Dias, G. M., Eggleton, B. J., Maguire, S., Maine, E., Malloy, T., Nathwani, J., Nazar, L., Sips, A., Sone, J., van den Berg, A., Weiss, P. S., & Mitra, S. (2021). Nanotechnology for a Sustainable Future: Addressing Global Challenges with the International Network4Sustainable Nanotechnology. *ACS nano*, *15*(12), 18608–18623. https://doi.org/10.1021/acsnano.1c10919.

Priya, M., Selvi, B. K., & Paul, J. A. (2011). Green synthesis of silver nanoparticles from the leaf extract of *Euphorbia hirta* and *Nerium indicum*. *Digest Journal of Nanomaterials & Biostructures*, 6, 869–877.

Rauf, M. A., Oves, M., Rehman, F. U., Khan, A. R., Husain, N. (2019). *Bougainvillea* flower extract mediated zinc oxide's nanomaterials for antimicrobial and anticancer activity. *Biomedicine & Pharmacotherapy*, 116, 108983. https://doi.org/10.1016/j.biopha.2019.108983.

Sharma, N., Khajuria, V., Gupta, S., Kumar, C., Sharma, A., Lone, N. A., Paul, S., Meena, S. R., Satti, N. K., & Verma, M. K. (2021). Dereplication based strategy for rapid identification and isolation of a novel anti-inflammatory flavonoid by LCMS/MS from *Colebrookea oppositifolia*. *ACS Omega*, 6(45), 30241–30259. https://doi.org/10.1021/acsomega.1c01837.

Sharma, R.K. & Ghose, R. (2015). Synthesis of zinc oxide nanoparticles by homogeneous precipitation method and its application in antifungal activity against *Candida albicans*. *Ceramics International*, 41(1), 967–975. https://doi.org/10.1016/j.ceramint.2014.09.016.

Shilpakar, R., Paudel, B. D., Sharma, R., Silwal, S. R., Sapkota, R., Shrestha, P., Dulal, S., Piya, M. K., Tuladhar, S. M., Neupane, P., Dhimal, M, Niraula, A., & Uprety, D. (2022). Lung cancer in Nepal. *Journal of Thoracic Oncology*, 17(1), 22–29. https://doi.org/10.1016/j.jtho.2021.10.020.

Shin, S. A., Moon, S. Y., Kim, W. Y., Paek, S. M., Park, H. H., & Lee, C. S. (2018). Structure- based classification and anti-cancer effects of plant metabolites. *International Journal of Molecular Sciences*, 19(9), 2651. https://doi.org/10.3390/ijms19092651.

Shobha, N., Nanda, N., Giresha, A. S., Manjappa, P., Sophiya, P., Dharmappa, K. K., & Nagabhusana, B. M. (2019). Synthesis and characterization of zinc oxide nanoparticles utilizing seed source of *Ricinus communis* and study of its antioxidant, antifungal and anticancer activity. *Materials Science and Engineering C*, 97, 842–850. https://doi.org/10.1016/j.msec.2018.12.023.

Shrestha, D., Budha Magar, A., Pakka, S., & Sharma, K. R. (2024). Phytochemical analysis, antioxidant, antimicrobial, and toxicity studies of *Schima wallichii* growing in Nepal. *International Journal of Food Properties*, 27(1), 273-285. https://doi.org/10.1080/10942912.2024.2304267.

Shrestha, D. K., Budha Magar, A., Bhusal, M., Baraili, R., Pathak, I., Joshi, P. R., Parajuli, N., & Sharma, K. R. (2024). Synthesis of silver and zinc oxide nanoparticles using *Polystichum lentum* extract for the potential antibacterial, antioxidant, and anticancer activities. *Journal of Chemistry*, 2024(1), 1876560. https://doi.org/10.1155/2024/1876560.

Shrestha, D. R., Jaishi, D. R., Ojha, I., Ojha, D. R., Pathak, I., Budha Magar, A., Parajuli, N., & Sharma, K. R. (2024). Plant assisted synthesis of silver nanoparticles using *Persicaria perfoliata* (L.) for antioxidant, antibacterial, and anticancer properties. *Heliyon*, 10(23), e40543. https://doi.org/10.1016/j.heliyon.2024.e40543.

Singh, K., Singh. J., & Rawat, M. (2019). Green synthesis of zinc oxide nanoparticles using *Punica granatum* leaf extract and its application towards photocatalytic degradation of Coomassie brilliant blue R-250 dye. *SN Applied Sciences*, 1(6), 624. https://doi.org/10.1007/s42452-019-0610-5.

Slavin, Y. N. & Bach, H. (2022). Mechanisms of antifungal properties of metal nanoparticles. *Nanomaterials*, 12(24), 4470. https://doi.org/10.3390/nano12244470.

Viswanatha, G. L., Shylaja, H., Kumar, H. Y., Venkataranganna, M. V., & Prasad, N. B. L. (2021). Traditional uses, phytochemistry, and ethnopharmacology of *Colebrookea oppositifolia*

Smith: a mini-review. *Advances in Traditional Medicine*, 21(2), 209–229. https://doi.org/10.1007/s13596-020-00513-y.

Wu, F., Harper, B. J., & Harper, S. L. (2019). Comparative dissolution, uptake, and toxicity of zinc oxide particles in individual aquatic species and mixed populations. *Environmental Toxicology and Chemistry*, 38(3), 591–602. https://doi.org/10.1002/etc.4349.

Yadav, S. & Maurya, P. K. (2021). Biomedical applications of metal oxide nanoparticles in aging and age-associated diseases. *3 Biotech*, 11(7), 338. https://doi.org/10.1007/s13205-021-02892-8.

Yassin, M. T., Elgorban, A. M., Al-Askar, A. A., Sholkamy, E. N., Ameen, F., & Maniah, K. (2023). Synergistic anticandidal activities of greenly synthesized ZnO nanomaterials with commercial antifungal agents against Candidal infections. *Micromachines*, 14(1), 209. doi: https://doi.org/10.3390/mi14010209.

Zak, A. K., Abrishami, M. E., Majid, W. H. A., Yousefi, R., & Hosseini, S. M. (2011). Effects of annealing temperature on some structural and optical properties of ZnO nanoparticles prepared by a modified sol-gel combustion method. *Ceramics International*, 37(1), 393–398. https://doi.org/10.1016/j.ceramint.2010.08.017.

Zhou, W. & Greer, H. F. (2016). What can electron microscopy tell us beyond crystal structures? *European Journal of Inorganic Chemistry*, 2016(7), 941–950. https://doi.org/10.1002/ejic.201501342.